Nat. Hazards Earth Syst. Sci., 10, 843–855, 2010
www.nat-hazards-earth-syst-sci.net/10/843/2010/

Natural Hazards and Earth System Sciences

Effects on atmospherics at 6 kHz and 9 kHz recorded at Tripura during the India-Pakistan Border earthquake

S. S. De[1], B. K. De[2], B. Bandyopadhyay[1], S. Paul[1], D. K. Haldar[1], A. Bhowmick[2], S. Barui[1], and R. Ali[3]

[1]S K Mitra Centre for Research in Space Environment, Centre of Advanced Study in Radio Physics and Electronics, University of Calcutta, Kolkata 700 009, India
[2]Department of Physics, University of Tripura, Agartala 799 130, India
[3]N. S. Mahavidyalaya, Udaypur, Tripura, India

Received: 24 September 2009 – Revised: 4 April 2010 – Accepted: 6 April 2010 – Published: 16 April 2010

Abstract. The outcome of the results of some analyses of electromagnetic emissions recorded by VLF receivers at 6 kHz and 9 kHz over Agartala, Tripura, the North-Eastern state of India (Lat. 23° N, Long. 91.4° E) during the large earthquake at Muzaffarabad (Lat. 34.53° N, Long. 73.58° E) at Kashmir under Pakistan have been presented here. Spiky variations in integrated field intensity of atmospherics (IFIA) at 6 and 9 kHz have been observed 10 days prior (from midnight of 28 September 2005) to the day of occurrence of the earthquake on 8 October 2005 and the effect continued, decayed gradually and eventually ceased on 16 October 2005. The spikes distinctly superimposed on the ambient level with mutual separation of 2–5 min. Occurrence number of spikes per hour and total duration of their occurrence have been found remarkably high on the day of occurrence of the earthquake. The spike heights are higher at 6 kHz than at 9 kHz. The results have been explained on the basis of generation of electromagnetic radiation associated with fracture of rocks, their subsequent penetration into the Earth's atmosphere and finally their propagation between Earth-ionosphere waveguide. The present observation shows that VLF anomaly is well-confined between 6 and 9 kHz.

1 Introduction

There are different models on seismic waves, e.g., ETAS Model (Epidemic Type After Shock model) (Ogata et. al., 1989), SPM (Stationary Poisson Model) (Console and Murru, 2001), EEPAS model (Every Earthquake a Precursor According to Scale) (Rhoades and Evison, 2004; Evison and Rhoades, 2001, 2004), PPE model (Proximity to Past Earthquake) (Jackson and Kagan, 1999) and on the generation of electric field within the upper atmosphere (Gokhberg et al., 1984; Kim and Hegai, 1997, 2002; Fujinawa and Takahashi, 1998) due to seismo-ionospheric coupling phenomena during the occurrence of any strong earthquake (Hayakawa, 1999; Hayakawa et al., 2004; Pulinets et al., 2003). The emission and propagation of electromagnetic waves from large earthquakes in the ULF-ELF-VLF bands have been reported (Gokhberg et al., 1982; Fujinawa and Takahashi, 1998). Both precursory and post-seismic variations in ELF-VLF amplitudes and in ionospheric parameters are well-known from satellite-based observations surrounding the earthquake zones (Pulinets, 1998; Shvets et al., 2002; Molchanov and Hayakawa, 1998; Calais and Minster, 1995; Liu et al., 2004). Electromagnetic anomalies (EA) before the destructive earthquake in Greece covering wide range of frequencies have been analyzed by Eftaxias et al. (2003). The paper asserts that EA are correlated with the fault model characteristics of the associated earthquake and with the degree of geotectonic heterogeneity within the focal zone. Using the in situ laboratory experiments of rupture and seismological arguments related to Kozani Grevena earthquake on 13 May 1995 in Greece (Lat. 40.2° N, Long. 21.7° E), pre-seismic very high frequency (VHF) and very low frequency (VLF) electromagnetic signals have been investigated (Kapiris et al., 2002). Spiky nature of electromagnetic signals at 3 kHz frequency is detected which is alike with the VLF pre-seismic signals of Kozani Grevena earthquake. In the observations of the 1995 Hyogo-Ken Nanbu earthquake, similar records at VLF frequencies are reported (Yamada and Oike, 1996; Nagao et al., 2002). Spiky signatures are also reported in the publications of other investigators (Ohta et al., 2001; Izutsu, 2007). Source to receiver

Correspondence to: S. S. De
(de_syam_sundar@yahoo.co.in)

Published by Copernicus Publications on behalf of the European Geosciences Union.

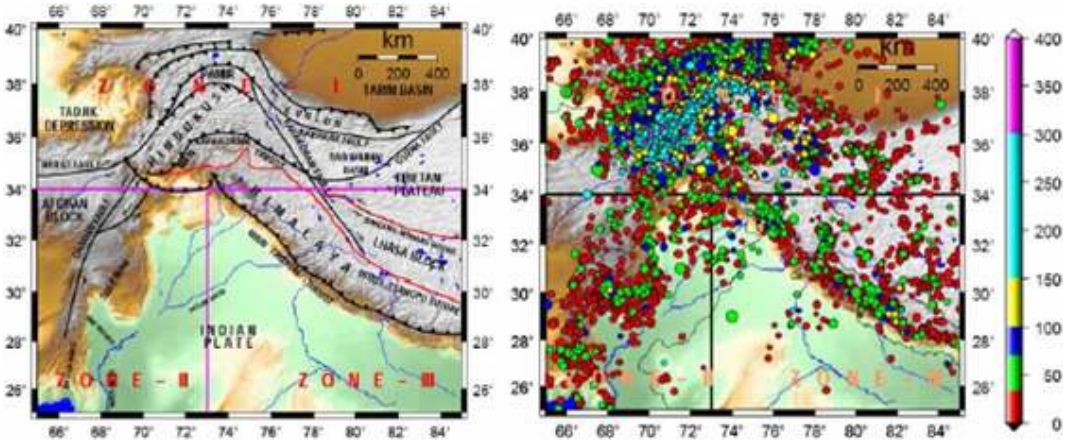

Fig. 1. It depicts tectonic map of three different regions (left figure) and seismicity map over three regions (right figure) showing vertical distribution of earthquakes during 1853–2005 (Shanker et al., 2007).

distances of these observations are quite large, results can not be supported by meteorological phenomena. The time evolution of sequences in EA revealed striking similarities to that observed in laboratory acousto- and electromagnetic emissions.

During the strong seismo-ionospheric coupling processes in the earthquake preparation zone, underground gas discharges carry submicron aerosols with them which enhance the intensity of electric field at the near ground due to the drop in air conductivity created by aerosols (Chemirev, 1997; Krider and Roble, 1986). Seismo-electromagnetic emissions have been observed at low frequency bands in the seismically active zones prior to the incidence of any large earthquake (Nagao et al., 2002) which are different from lightning induced and technogenic emissions. On the event of strong earthquakes, the near ground of the atmospheric layer becomes ionized and generates strong electric field which introduces particle acceleration thereby exciting local plasma instabilities.

Ion cluster mass and plasma concentration during the process of lithosphere-ionosphere coupling vary with the vastness of the earthquake. As a result, the seismo-electromagnetic emissions would be expected to cover almost the whole of ULF-ELF-VLF band. In the process, there will be increase of thermal plasma noise along with other types of emissions, e.g., Cerenkov, and Bremstrallung. This sort of plasma instability at the surface may be assumed to be simulated in dusty plasma (Kikuchi, 2001).

The Himalayas laterally extends for about 2400 km from Western Kashmir to the Indo-Barman border. The ongoing convergences between the Indian and Eurasian pates has resulted in a very high level of seismicity in this region. In this area of convergence, transpressional tectonics also seems to be operative. A large number of faults have been recognized in the North-West Himalaya of Pakistan. These include faults of very large extent, such as the Main Mantle Thrust (MMT), the Main Boundary Thrust (MBT) and the Himalayan Frontal Thrust (HFT), as well as local faults. According to the map of faults, there are at least 41 active faults in the belt of North-West Himalayas (MonaLisa et al., 2006, 2007, 2008). The Himalayan part of the Alpine belt and its neighbouring region, including India, Pakistan, Afghanistan, Hindukush, Pamirs, Mangolia and Tien-Shan, bounded by 25°–40° N and 65°–85° E, have been considered for seismic risk assessment. The region is divided into three distinct tectonic zones based on seismic activity. Zone I is bounded by 34°–40° N and 65°–85° E. Zone II is bounded by 25°–34° N and 65°–73° E. Zone III is within 25°–34° N and 73°–85° E. The regions are shown in Fig. 1 (left side). The Fig. 1 also shows the vertical distribution of earthquakes (right side).

The 8 October 2005, Muzaffarabad-Kashmir earthquake was the deadliest in the history of the Indian sub-continent that killed more than 80 000 people. It occurred at 08:50:38 Pakistan Standard Time on 8 October 2005. The strength is M 7.7 with its epicenter at Lat. 34.53° N, Long. 73.58° E, about 19 km NE of Muzaffarabad and 100 km NE of Islamabad. The depth of the epicenter of the main shock is 26 km whereas the depth of aftershocks are distributed between 5–20 km, among which most are of depth 10 km. The earthquake occurred in a rupture plane 75 km long and 35 km wide (Pathier et al., 2006; Avouac et al., 2006). About 147 aftershocks have been documented on the first day after the initial shock, one of which has a magnitude of 6.4. Twenty eight occurred with magnitude greater than M=5 during four days after the main event (MonaLisa et al., 2008). On 19 October 2005, there was a series of strong aftershocks, one with a magnitude M=5.8 occurred about 65 km North of North-West of Muzaffarabad.

In this paper, the results of some significant observations at 6 kHz and 9 kHz recorded over Agartala (Lat. 23° N, Long. 91.4° E) by VLF receivers during the India-Pakistan border earthquake occurred on 8 October 2005, at Kashmir (under

Table 1. Cut-off frequency of low-pass filter and corresponding tuned frequency.

Cut-off frequency (Low-Pass Filter) kHz	Tuned frequency kHz
3	0.900 (in lieu of 1)
5	3
8	6
12	9
15	12

Pakistan) will be presented. The effects of the vast earthquake (M: 7.6) are exhibited through the occurrence of discrete spikes. Numbers of spikes were observed first on 28 September 2005 and continued up to 13 October 2005. Both number of spikes and their intensities as well as durations were found to be changed irregularly and reached the maximum value on the day of occurrence. The signatures ceased gradually and almost ended after 13 October 2005. These commencements may be considered to be precursory and post-seismic effects of this vast earthquake. The records were taken at Agartala which is about 2179 km away from the place of occurrence. The effects at 6 kHz have been found to be more prominent than at 9 kHz records. Observations were taken at Agartala continuously at frequencies 1, 3, 6, 9 and 12 kHz. No such effects had been observed except at 6 kHz and 9 kHz. The data were analyzed and the outcome of the results will be presented.

2 Instrumentation

The VLF spectra of different frequencies 1, 3, 6, 9 and 12 kHz are regularly recorded over the last several years from Agartala (Lat. 23° N, Long. 91.4° E). The signals are processed and are being recorded in a computer. The RMS values of the filtered data are analyzed regularly using Origin 5.0 software.

The receiver system mainly consists of (a) Antenna (b) AC amplifier (c) Selective circuit (d) Detective circuit (e) Logarithmic amplifier, and (f) Recording device. The receiver system is presented in Fig. 2 through flow chart. The effective height of antenna is fixed to 8.63 m and the terminal capacitance of the antenna wire is kept at 694 pF.

The experimental set-up, installed at the Tripura University site of Agartala, consists of an inverted L-type antenna to receive vertically polarized atmospherics in the ELF-VLF bands from near and far sources. By selecting the bands, unwanted noise has been reduced. The cut-off frequencies of the low-pass filter and tuning frequencies are different. As for example, to receive atmospherics at 3 kHz, the antenna induced voltage is passed through a low-pass filter with a cut-

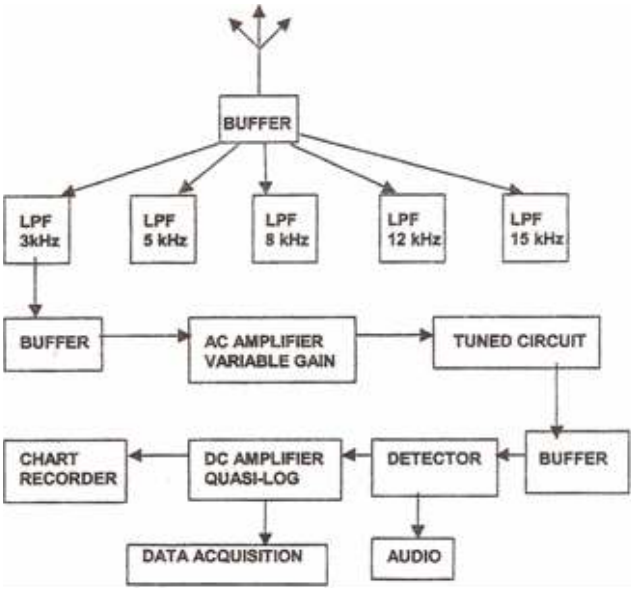

Fig. 2. Flow chart of the ELF-VLF receiving system at Agartala (Lat. 23° N, Long. 91.4° E).

off frequency of 5 kHz as shown in Table 1. The filter output is amplified with an AC amplifier using OP AMP IC531 in a non-inverting mode. The gain has been limited within the value to check transients that may trigger sustained oscillations in the amplifier. The amplifier is followed by a series resonant circuit tuned to the desired frequency and a buffer. The selective circuit is a series combination of an inductance and a capacitance.

To ensure high selectivity, the inductive coil is mounted inside a pot-core of ferrite material. The selected sinusoidal Fourier components of atmospherics are then passed to the input of a detector circuit through a unit gain buffer using OP AMP IC531. In the detector circuit, the diode OA79 is used in the negative rectifying mode. The output of the diode is across a parallel combination of resistance and capacitance, so that, the detecting time constant would be 0.22 s. The level of the detected envelope is proportional to the RMS value of the Fourier component.

The detected RMS output is amplified by a quasi-logarithmic dc amplifier using OP AMP 741 in the DC mode of operation. The calibration of the recording system has been done using a standard signal generator with an accuracy of ± 0.86 dB. During calibration, the antenna was disconnected from the filter circuit and replaced by the signal generator through a capacitance having a value equal to the terminal capacitance of the antenna. At first, the outputs are calibrated in terms of RMS value of induced voltages at the antenna. To get very low signals from the function generator, a dB-attenuator is used. The output is calibrated in terms of values of dB above 1 μV. Then it is converted to an absolute RMS value in units of μV. The absolute value of induced

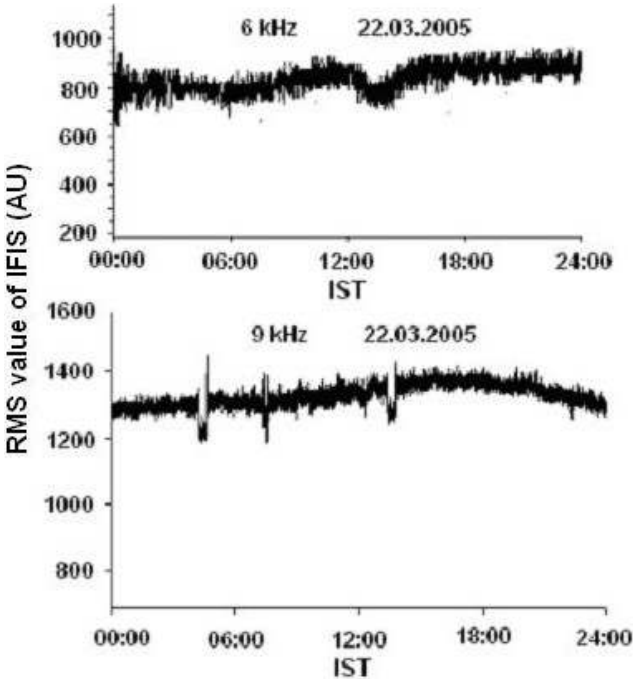

Fig. 3. A normal day record of sferics at 6 kHz and 9 kHz in a meteorologically clear day.

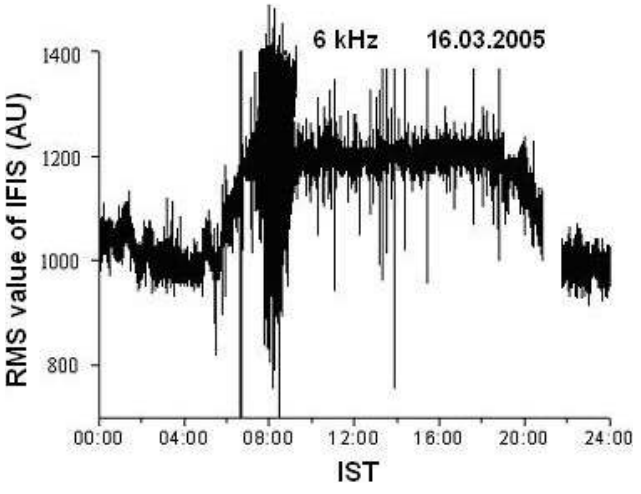

Fig. 4. A record of IFIS on a rainy day with overhead shower 07:10 to 09:15 IST.

voltage has been divided by the effective height of the antenna to calculate the field strength in μV/m.

The data in the form of RMS value are recorded by digital technique using a data acquisition system. The digital data acquisition system uses a PCI 1050, 16 channel 12 bit DAS card (Dynalog). It has a 12 bit A/D converter, 16 digital input and 16 digital output. The input multiplexer has a built-in over-voltage protection arrangement. All the I/O parts are accessed by 32 bit I/O instructor, thereby increasing the data input rate. It is supported by a powerful 32-bit API, which functions for I/O processing under the Win 98/2000 operating system. The detected RMS voltage has been sampled out at the rate of 1 Hz.

3 Observations and interpretations

From the VLF sferics at 1, 3, 6, 9 and 12 kHz, which are simultaneously recorded at Agartala (Lat. 23° N, Long. 91.4° E) round-the-clock, various features are observed. The monsoon record is highly different from winter records. The difference between daily maximum and daily minimum is of the order of 12–16 dB in monsoon whereas it is 8–13 dB in winter. Data have been collected since February 2005 to January 2008 (three-year period). During our atmospheric monitoring period we observed spikes in IFIA in relation to Muzaffarabad earthquake. Figure 3 depicts the raw data of sferics at 6 and 9 kHz in a meteorologically clear day. Data of 10 months are examined for a period from February 2005 to November 2005 in order to compare the observed anomaly with the period of thunder activity. In the records of integrated field intensity of sferics (IFIS) and even during the period of local rain or overhead shower, spikes are not observed (Fig. 3). Figure 4 exhibits the records of overhead shower occurred from 07:10 to 09:15 IST on 16 March 2005, where it shows no spikes during the period. Figure 5 represents the record of IFIS on 16 June 2005. Rain occurred within a radius of 10–15 km and partially overhead rain occurred along with lightning during 14:15 to 16:05 IST. The record does not exhibit spikes during the period. The record of IFIS on a day, thunderstorms occurred in south Tripura at a distance of about 40–50 km from the receiving station which are presented in Fig. 6, where spikes are not seen. Typical records of IFIS at 6 and 9 kHz during a thunderstorm at North Tripura at a distance of 75–100 km is given in Fig. 7. The arrow mark indicates the onset of rain. Figure 8 shows the enhancement of IFIS during a thunderstorm occurring about mid-day. In the case of distant cloud activity, the level of integrated field intensity of sferics increases. From the data of distant lightning activity for 10 months, it is found that it can only change the level of IFIS and transient variation of sferics signals.

But, some days prior to the vast earthquake at Muzaffarabad (Lat. 34.53° N, Long. 73.58° E) on 8 October 2005, remarkable spiky variations at 6 kHz and 9 kHz records are observed. In the time scale, spikes occur in the duration of the order of a few minutes. If the recorded data of 24 h is shown in a full paper, the variation of duration of a few minutes will appear as spikes. The nature of spikes is completely different from the transient variation occurred due to local or far thunderstorms. The rate of sampling of 1 Hz of the DC level is sufficient to detect variation of duration of a few minutes. The spike-heights are high compared to that of ambient spikes of transient variations in sferics sources. Dominant spikes are found to appear first during midnight

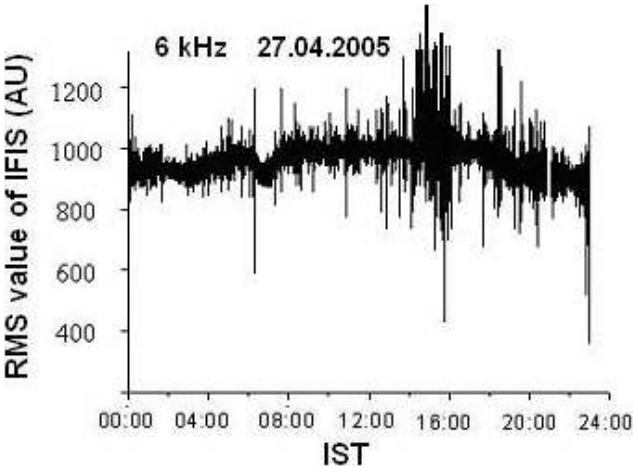

Fig. 5. A record of IFIS on a rainy day with overhead shower 14:15 to 16:05 IST.

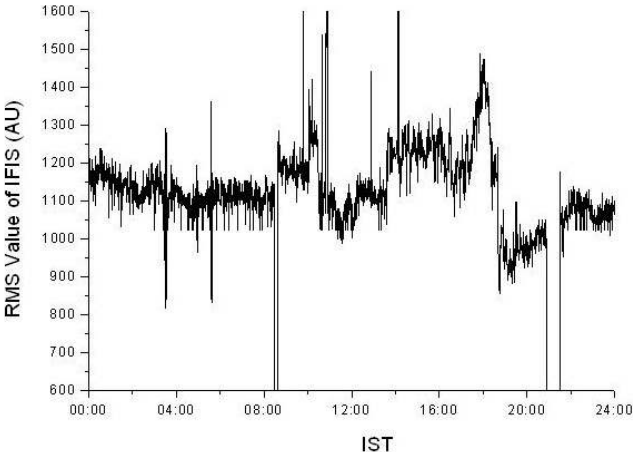

Fig. 6. A record of IFIS in relation to thunderstorm activity in south Tripura at a distance 40–50 km from the receiving station.

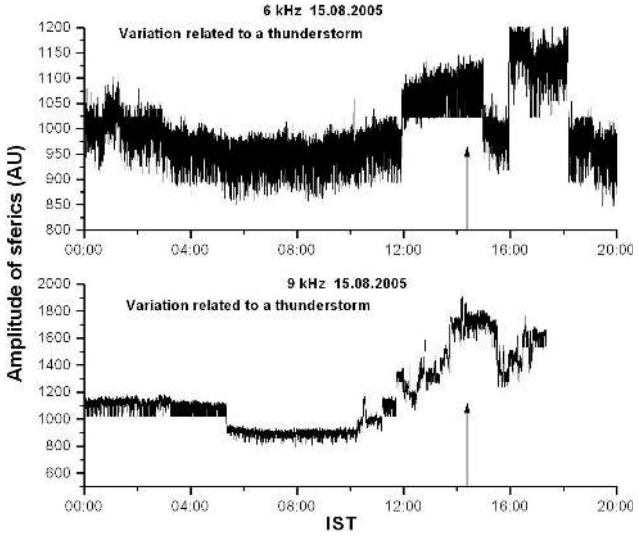

Fig. 7. A typical record of sferics at 6 kHz and 9 kHz during a thunderstorm over North Tripura at a distance 75–100 km. The arrow mark indicates the onset of rain associated with thunderstorm.

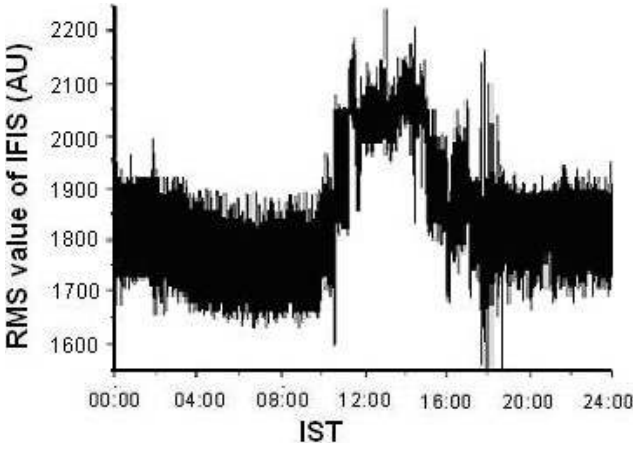

Fig. 8. A typical record of sferics at 6 kHz during a thunderstorm over North Tripura at a distance 75–100 km.

on 28 September 2005 (Fig. 9). These large spikes also appeared prominently on 5 October 2005 only in the records of 6 and 9 kHz frequencies which are shown. Number of dominant spikes and duration of their occurrence are found to increase till they showed maximum value on the day of occurrence of the earthquake. The meteorological data has been mentioned here to indicate the fact that even nearby thunderstorms having distance <100 km do not produce distinct spikes in IFIA. So presence of spikes cannot be due to any thunderstorm activity in global scale. This is one supporting reason that the spikes should be due to extra-VLF emission from the earthquake epicenter, then propagating to the surface of the Earth. The appearance of spikes were initially doubtful whether these are the signatures of a geophysical phenomena or local noise. The first point is that the experimental site has been selected to keep the receivers away from the man-made noise. The experimental site is in rural place, 10–12 km away from the nearest town. So, there is no question of man-made noise. The electric wiring in the concerned building were thoroughly checked to detect any fault which could have produced discharge giving spikes in the record. No such fault was present there. The spikes are in some cases present during post mid-night. At post mid-night, there cannot be any possibility of man-made noise since the locality is purely a rural place, free from even small and large industries. It is worth-mentioning that occasionally a few isolated spike-type noise signals, i.e., transients are present in the records and these were due to operation of electrical equipments. The nature of these transients and their chracteristic separations are completely different from various known effects, e.g., solar flare effect, meteor shower

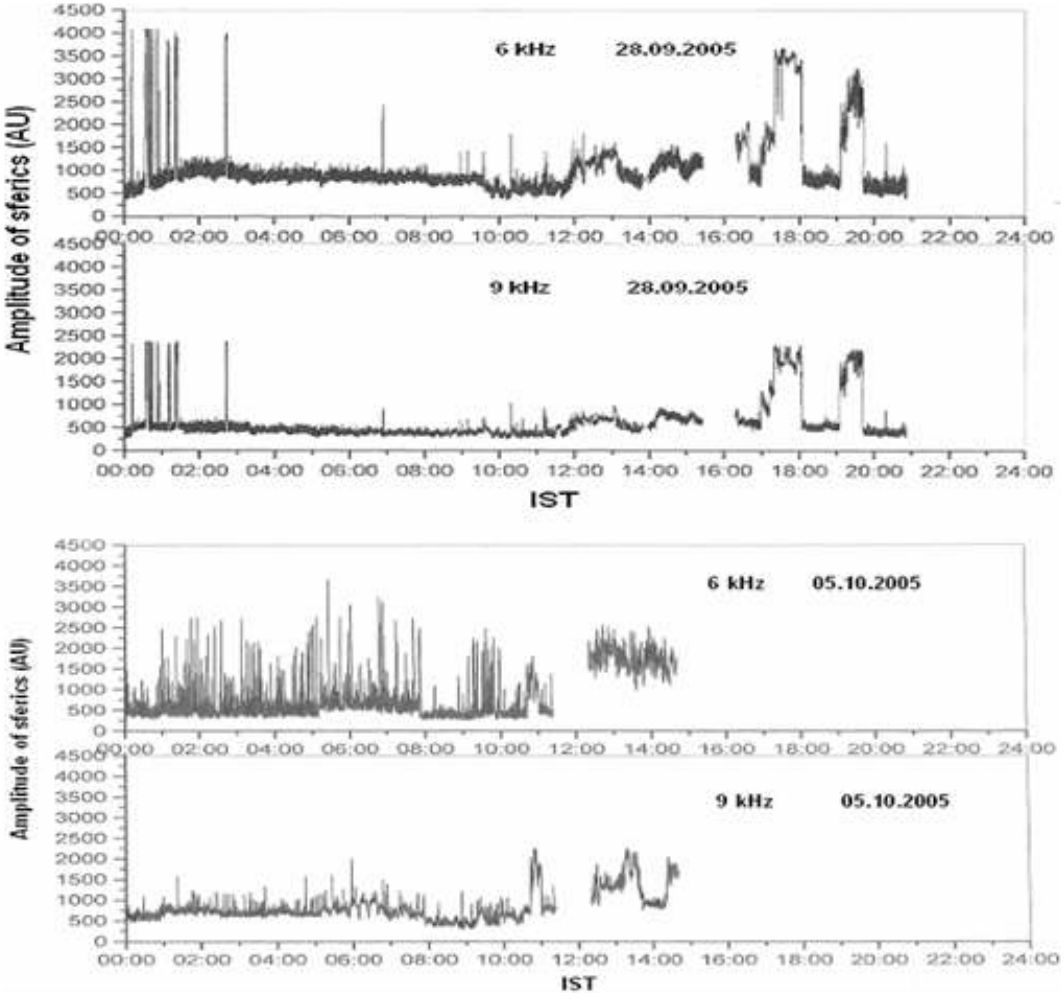

Fig. 9. Diurnal variations of sferics observed over Agartala. Upper two records are at 6 and 9 kHz on 28 September 2005. The records show typical spikes beginning around midnight. The lower two graphs show the existence of spikes on 5 October 2005.

effect, geomagnetic storms. Between 28 September 2005 and 18 October 2005, there were no meteorological phenomena such as thunderstorm or cyclone or heavy shower on the path between Muzaffarabad (Lat. 34.53° N, Long. 73.58° E) and Agartala (Lat. 23° N, Long. 91.4° E). Only there were some scattered thundershowers after 22:00 IST of 8 October 2005 to the midnight, 02:00 IST. This has been confirmed by the weather report from website. The difference can be realized from the comparison of Figs. 4 to 8 with other figures from 9 to 12. Figures 4 to 8 show variation in sferics at 6 and 9 kHz due to thunderstorm activity and the Figs. 9 to 12 show spiky variations associated with the earthquake. In the cases of earthquake related events, the spikes maintain an interval of the order of 2–5 min on an average. The spikes produced by thunderstorms are associated with remarkable variations in base level and spikes are also extended downward. The spikes related to earthquakes are distinct from each other and the base level remains almost constant and not extended downward.

Number of spikes per hour above the ambient level was found to be very large and the height of spikes above the ambient value is also remarkably high. The huge magnitude of spikes commenced a few days prior to the day of occurrence of the earthquake. It may be realized as the precursors of the earthquake. The intensity of spikes gradually reduced and almost ceased after 13 October 2005. The effects at 6 kHz have been found to be remarkably high than at 9 kHz.

Some typical features of the records during the period between 28 September 2005 and 18 October 2005, are presented in Figs. 9 to 12. The spectral analyses of the recorded data for the period considered are given. The results are shown in Table 2.

The variations of spike intensity per hour before and after the earthquake have been depicted by bar graphs (Figs. 13–14). It is seen that on the day of occurrence, the response at 6 kHz is much higher than at 9 kHz. Both precursory and post-earthquake effects are found to be different at these two frequencies.

Table 2. Statistical analyses of different characteristic parameters of the earthquake from the recorded data.

Date	Frequency (kHz)	Duration of occurrence of spikes in hour	Ambient level of spikes (AU)	No. of spikes above the ambient levels	Average height of spikes (AU)	Total no of spikes	Average height of all the spikes above the ambient level of spikes
28/09/05	6	00:00–15:26 16:19–20:46	1570 1570	9 4	3045 3390	13	1647
	9	00:00–15:26 16:19–20:46	1055 1055	8 4	2200 2275	12	1182
29/09/05	6	16:19–20:46	1728	2	3574	2	1846
	9	00:00–15:26 16:19–20:46	1730 1280	1 2	1880 2065	3	467.5
30/09/05	6	10:55–18:35 21:57–23:59	1415 840	12 1	3390 1205	13	1170
	9	10:55–18:35	1610	8	2625	8	1015
01/10/05	6	00:00–01:57 09:02–09:23 09:25–13:08 13:10–14:33 15:36–17:28 18:49–21:24 23:34–23:59	2080 2965 1765 2275 1075 775 805	1 1 16 6 5 4 1	4015 3980 2405 2995 2695 1830 2870	33	1672
	9	00:00–01:57 09:02–09:23 09:25–13:08 13:10–14:33 15:36–17:28 18:49–21:24	1305 1495 1565 1025 755 670	1 2 2 6 2 1	4105 2105 1940 1960 1335 1545	14	882
02/10/05	6	00:00–00:46 04:24–11:22 11:22–23:51	1840 1840 1690	1 28 9	2935 3475 201	38	1042
	9	00:07–08:19 08:19–23:48	1417 1940	10 6	1971 1987	16	300
03/10/05	6	00:05–09:47 12:00–17:31	1860 1475	26 14	2945 2310	40	960
	9	00:00–09:53 11:54–17:31	1485 1465	9 3	2035 1975	12	530
04/10/05	6	00:00–13:31 17:16–19:01 23:06–23:59	1505 1610 1975	24 4 1	2415 2270 2185	29	593
	9	00:00–13:26 17:14–19:03	1680 1845	17 5	1875 2415	22	383
05/10/05	6	00:00–11:28	1430	30	2350	30	920
	9	00:00–11:28	1358	5	1440	5	55
06/10/05	6	11:23–16:05 16:06–23:51	1560 1306	6 4	1781 1813	10	364
	9	16:27–19:25 20:19–23:59	1515 1405	1 4		5	365

Table 2. Continued.

Date	Frequency (kHz)	Duration of occurrence of spikes in hour	Ambient level of spikes (AU)	No. of spikes above the ambient levels	Average height of spikes (AU)	Total no of spikes	Average height of all the spikes above the ambient level of spikes
07/10/05	6	00:09–09:06 18:26–23:51	1215 1250	14 3	2345 1520	17	700
	9	00:09–09:06 18:26–23:51	1050 1650	9 3	1250 1860	12	205
08/10/05	6	00:00–23:59	1090	73	2650	73	1560
	9	00:00–23:59	1315	14	1535	14	220
09/10/05	6	00:00–15:45	1145	19	2190	19	1045
	9	00:00–15:45 17:34–23:59	1500 1500	7 1	2130 2105	8	617
10/10/05	6	No spikes					
	9	00:00–16:42 16:44–23:59	1730 1730	28 28	2295 2295	28	565
11/10/05	6	00:00–22:58	1034	13	2310	13	1276
	9	00:00–22:58	1540	5	1960	5	420
12/10/05	6	00:00–23:59	1115	4	1860	4	745
	9	00:00–23:59	1400	5	1775	5	375
13/10/05	6	00:00–23:59	1065	1	1125	1	60
	9	00:00–23:59	1400	1	1460	1	60
14/10/05	6	00:00–19:45	1065	2	1165	2	1010
	9	00:00–19:45	1265	2	1535	2	270
15/10/05	6	10:09–12:23 14:26–23:59	1160 1160	1 4	1500 1500	5	340
	9	14:26–23:59	1370	2	1820	2	450
16/10/05	6	00:00–15:58 15:59–16:55 16:58–23:59	1110 1670 1110	12 3 5	1890 2205 1260	20	488
	9	00:00–04:22 08:11–16:50 16:51–23:59	1000 1680 1090	2 9 3	1400 2050 175	14	485
17/10/05	6	02:27–07:15 07:19–16:13 23:25–23:59	1375 1040 730	1 3 2	1625 1305 1895	6	560
	9	09:49–10:34	1245	1	1380	1	135
18/10/05	6	00:00–09:25 09:49–10:34 10:42–20:59	1055 2205 1075	1 4 4	2270 2955 1575	9	821
	9	00:00–09:25 09:49–10:34 10:42–20:59	1295 1880 1290	1 4 3	1630 2285 1305	8	242

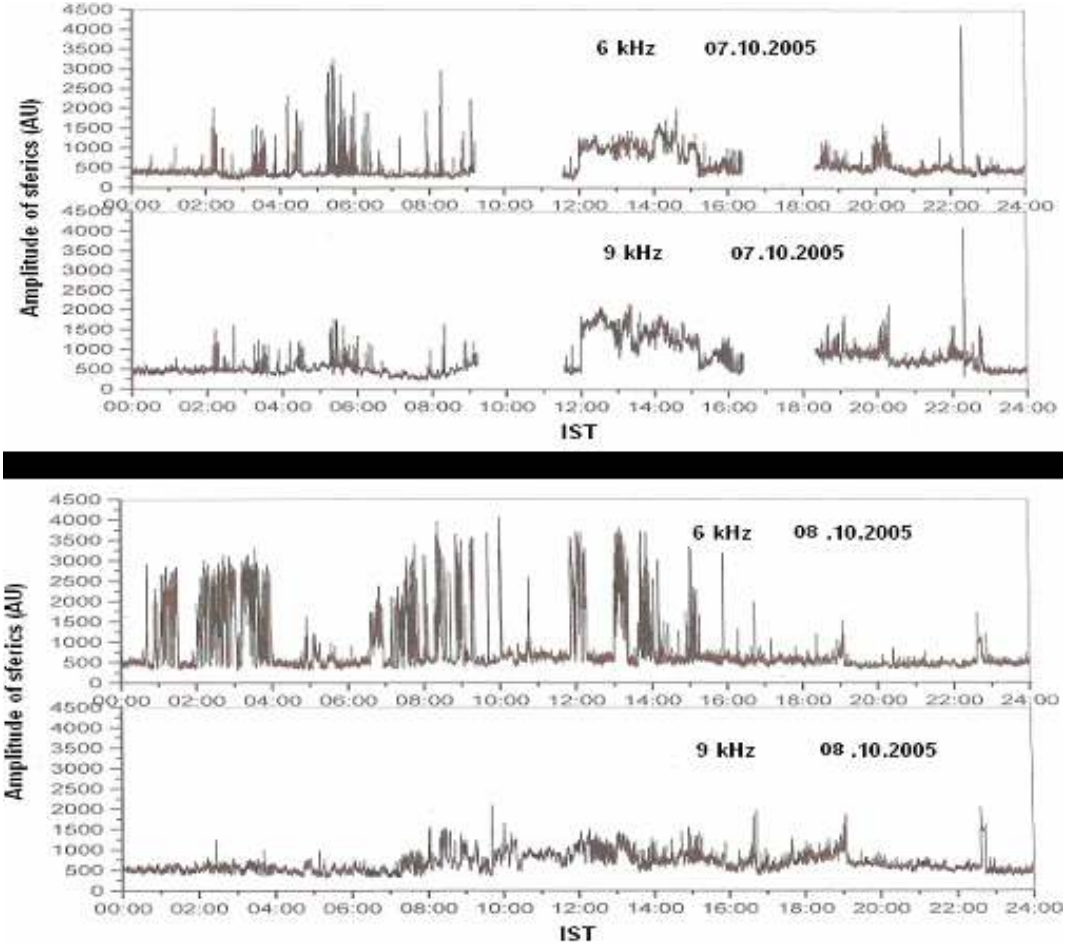

Fig. 10. Diurnal variation of sferics with spikes observed over Agartala on 7 October (upper two records) and 8 October 2005 (lower two records).

4 Discussion

Gokhberg et al. (1979) observed anomalous increases in electromagnetic radiation at 27 kHz, 385 kHz and 1.63 MHz before a large main shock (M: 7.4) of the Iran earthquake in a tunnel of 50 m below the ground in Caucasus. Gokhberg et al. (1982) also observed similar increase in electromagnetic radiations at 81 kHz before some earthquakes. In laboratory experiments, electromagnetic radiation associated with fractures of rocks has been detected (Ogawa et al., 1985). The occurrence of anomalous electromagnetic noises at 163 kHz for a few hours to several days before and after the main shocks of shallow earthquakes in island areas or shallow sea regions are reported (Oike and Ogawa, 1986). Impulsive electromagnetic noise bursts of seismogenic emission at 82 kHz and 1.525 kHz are recorded at frequencies below 1.5 kHz prior to earthquake (Takeo et al., 1992; Gokhberg et al., 1982). All these observations and analyses of seismogenic emissions are found to be related to large rock crushes (Yoshino, 1989). The penetration characteristics of electromagnetic emissions from an underground seismic source into the atmosphere, ionosphere and magnetosphere have been thoroughly discussed (Molchanov et al., 1995). A report of pulse-like electromagnetic signals associated with earthquakes in the frequency range 1–10 kHz is given by Asada et al. (2001). The association of the VLF emissions with the occurrences of earthquake is inferred from temporal correlation study between the direction of arrival of VLF signal and that of the epicenter. With four cases, the maximum of VLF activity was found during 1–4 days before the earthquake. The fact that the time of maximum VLF emission does not coincide with time of maximum shock in earthquake must be considered to constitute an important information in the VLF emission mechanism.

Underground water diffusion in a region associated with deformation of the crust prior to earthquake raises the electrical conductivity in the crust (Ishido and Mizutani, 1981). Thus in order to explain the electromagnetic radiation associated with earthquakes and volcanic activities, one has to calculate the attenuation of ELF/VLF waves in dry crust and wet soil.

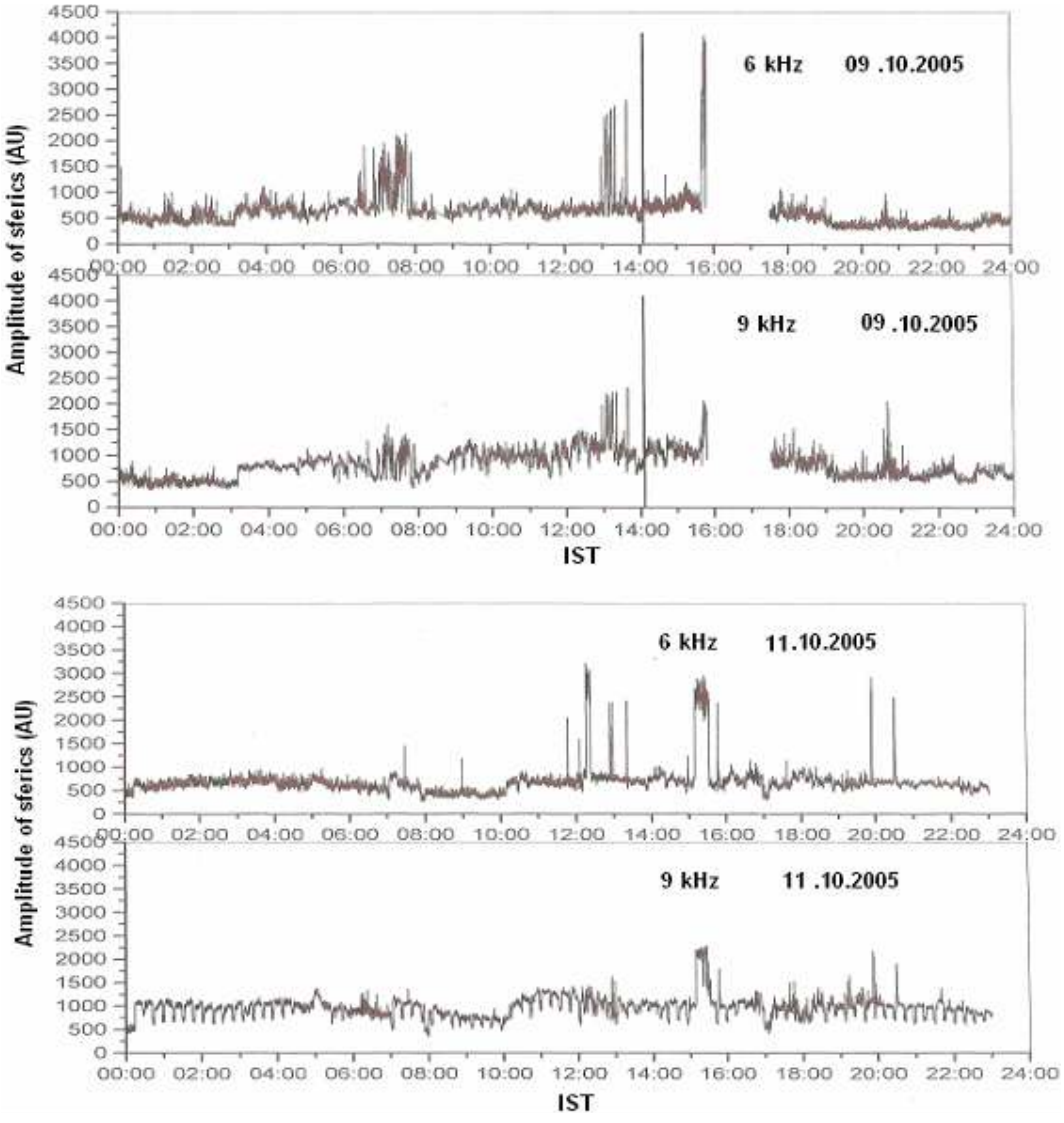

Fig. 11. Diurnal variation of sferics with spikes observed over Agartala on 9 October (upper two records) and 11 October 2005 (lower two records).

The electric field of electromagnetic waves may be expressed as

$$\boldsymbol{E} = \boldsymbol{E}_0 \exp\{j(\omega t + \boldsymbol{k}\cdot\boldsymbol{r})\} \quad (1)$$

where $\boldsymbol{k}$ is the wave vector given by $k^2 = \varepsilon\mu\omega^2 - j\sigma\mu\omega$, where ω is the angular wave frequency; $\boldsymbol{r}$, the radial vector from the radiation source; μ, the permeability; ε, the dielectric constant and σ is the electrical conductivity. The complex wave number is given by $\boldsymbol{k} = \alpha + j\beta$, $(\alpha > 0, \beta \geqq 0)$, α represents the propagation constant and β is the attenuation constant. The attenuation constant is derived as

$$\beta = \omega\left\{\varepsilon\mu/2\left(\sqrt{1+(\sigma/\varepsilon\omega)^2}\right) - 1\right\}^{1/2} \quad (2)$$

$\equiv (\sigma\mu\omega/2)^{1/2} = 1/\delta$ for $\sigma/\varepsilon\omega \gg 1$, where δ is the skin depth. The dielectric constant is expressed by $\varepsilon = \varepsilon_o\varepsilon_r$, where $\varepsilon_o = 1/(36\pi \times 10^9) F/m$ is the dielectric constant or permittivity of free space and ε_r is the relative permittivity. The magnetic permeability μ is usually approximated by the permeability of vacuum $\mu_o = 4\pi \times 10^{-7} H/m$, if the material concerned is not ferromagnetic. Relative permittivities ε_r of the material concerned are as follows: 1 for gas, 80 for water at 20 °C, and 55 for water at 100 °C. The electric conductivities σ of the material concerned are as follows: 10^{-2} mho/m for wet soil and 10^{-5} mho/m for dry crust. The expression of $\beta = 1/\delta$ can be properly used for electromagnetic wave attenuation below 100 kHz in wet soil and below 10 kHz in dry crust. For frequencies from 100 Hz to 10 kHz, the attenuation of electromagnetic waves in dry crust is less than 4 dB/km,

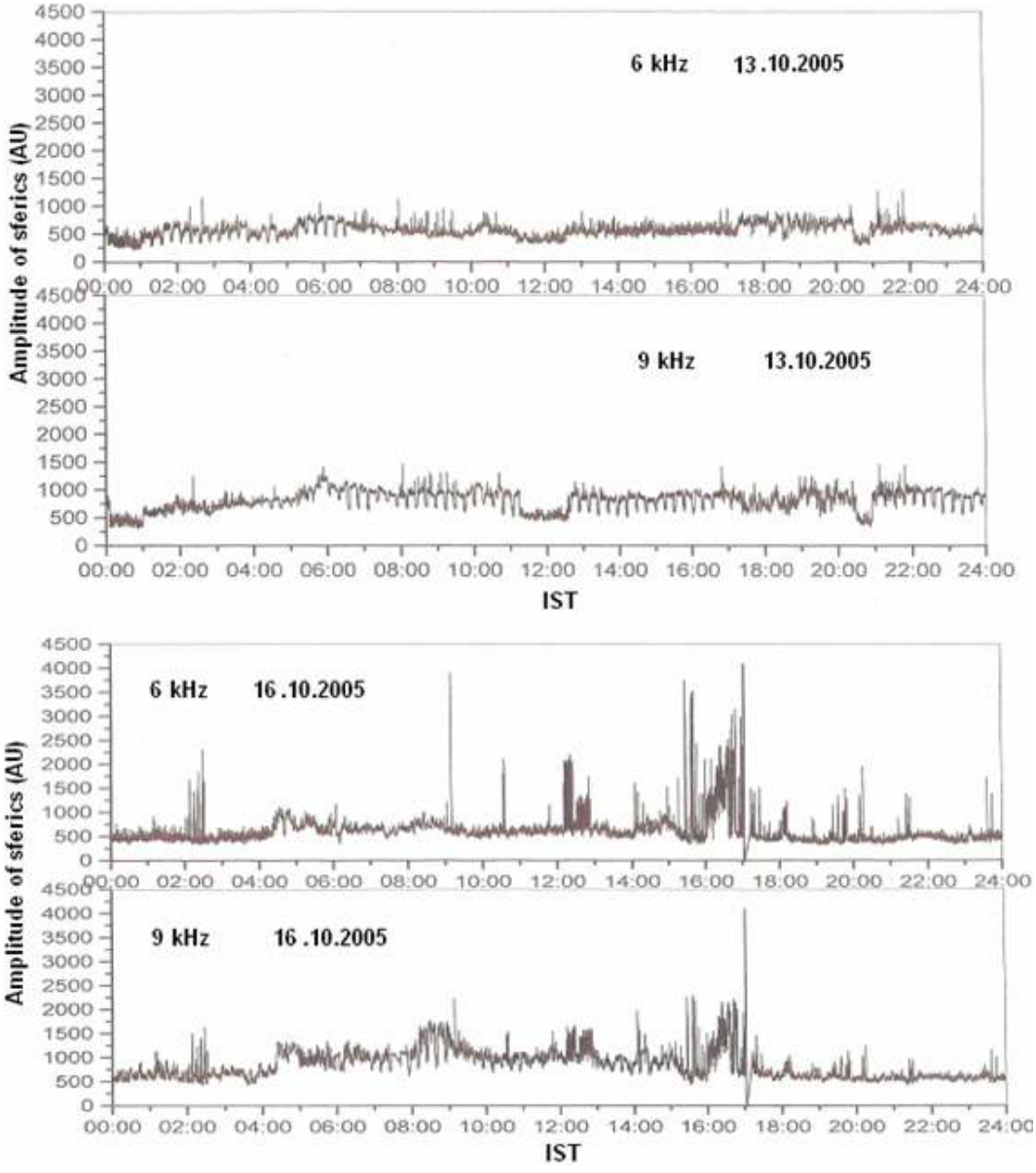

Fig. 12. Diurnal variation of sferics observed over Agartala on 13 October (upper two records) and 16 October 2005 (lower two records).

while it is from 17.3 dB/km at 100 Hz and above 100 dB/km at 1 kHz in wet soil. Therefore, if electromagnetic radiation is generated in dry crust by rock fractures over a vast region before and after the main shock of a shallow earthquake, anomalous electromagnetic waves will be observed even in the VLF band.

The present observation is only confined at 6 kHz and 9 kHz. The poor presence of spikes below at 1 and 3 kHz is probably due to much propagational attenuation of these frequencies in the Earth-ionosphere waveguide.

5 Conclusion

From the present study we may draw the following conclusions:

1. The generation of EM waves prior to and during severe earthquakes can produce spiky variations in IFIA at the receiving station at distances of the order of a few thousand km. The morphological structures of spikes are the characteristic feature related to earthquakes.

2. In the case of dry earth crust, only upto 10 kHz frequency of EM wave generated in the shock region can come upto the surface without much attenuation.

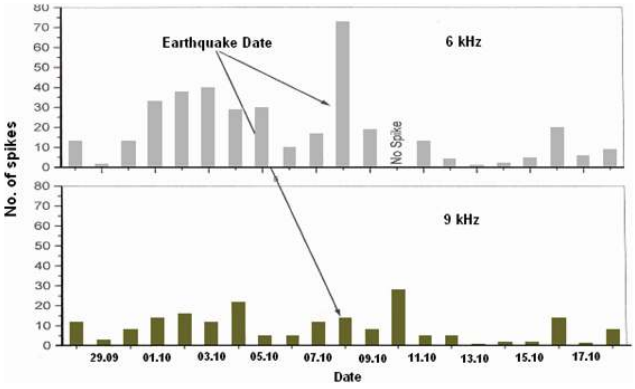

Fig. 13. Variation of spike intensity before and after the earthquake.

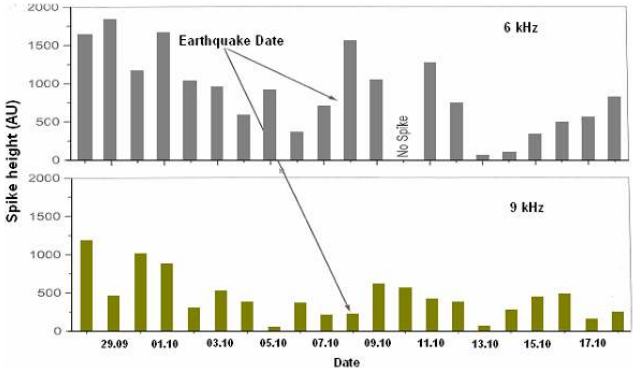

Fig. 14. Variation of spike heights above the ambient level before and after the earthquake.

After that EM waves launched into the Earth-ionosphere waveguide in which the 6 kHz and 9 kHz are less attenuated compared to 1 and 3 kHz.

3. The paths from after-shock regions to the Earth's surface are different for different hypocenters, and the strengths of different after-shocks are different. So, the uneven distributions in intensity of spikes are observed as in Figs. 13–14.

Acknowledgements. The authors acknowledge with thanks the financial support from Indian Space Research Organization (ISRO) through S K Mitra Centre for Research in Space Environment, University of Calcutta, Kolkata, India for carrying out the study. Figure 1 is taken from the work of Shanker et al. which is duly acknowledged.

Edited by: M. E. Contadakis
Reviewed by: D. Shanker and another anonymous referee

References

Armbruster, J. G., Seeber, L., and Jacob, K. K.: The northwest termination of the Himalayan mountain front: Active tectonics from micro earthquakes, J. Geophys. Res., 83, 269–282, 1978.

Asad, T., Baba, H., Kawazoe, M., and Sugiura, M.: An attempt to delineate very low frequency electromagnetic signals associated with earthquakes, Earth Planets Space, 53, 55–62, 2001.

Avouac, J. P., Ayoub, F., Leprince, S., Konca, K., and Helmberger, D. V.: The 2005 Mw 7.6 Kashmir earthquake: Sub-pixel correlation of ASTER images and seismic wave from analysis, Earth Planet. Sci. Lett., 249, 514–528, 2006.

Calais, E. and Minster, J. B.: GPS detection of ionospheric TEC perturbations following the January 17, 1994, Northridge Earthquake, Geophys. Res. Lett., 22, 1045–1048, 1995.

Chemirev, V. M., Isaev, N. V., Serebryakova, O. N., Sorokin, V. M., and Sobolev, Y. P.: Small-scale plasma inhomogeneities and correlated ELF emissions in the ionosphere over an earthquake region, J. Atmos. Solar-Terr. Phys., 59, 967–974, 1997.

Console, R. and Murru, M.: A simple testable model for earthquake clustering, J. Geophys. Res., 106B, 8699–8711, 2001.

Eftaxias, K., Kapiris, P., Polygiannakis, J., Peratzakis, A., Kopanas, J., Antonopoulos, G., and Rigas, D.: Experience of short term earthquake precursors with VLFVHF electromagnetic emissions, Nat. Hazards Earth Syst. Sci., 3, 217–228, 2003, http://www.nat-hazards-earth-syst-sci.net/3/217/2003/.

Evison, F. F. and Rhoades, D. A.: Model of long term seismogenesis, Ann. Geofis., 44, 81–93, 2001.

Evison, F. F. and Rhoades, D. A.: Demarcation and scaling of long term seismogenesis, Pure Appl. Phys, 161, 21–45, 2004.

Fujinawa, Y. and Takahashi, K.: Electromagnetic radiations associated with major earthquakes, Physics of the Earth and Planetary Interiors, 105, 249–259, 1998.

Gokhberg, M. B., Morgounov, V. A., and Aronov, E. L.: On high frequency electromagnetic radiation during seismic activity, Dokl. Akad. Nauk., 248, 1077–1087, 1979.

Gokhberg, M. B., Morgounov, V. A., Yoshino, T., and Tomizawa, I.: Experimental measurement of electromagnetic emissions possibly related to earthquake in Japan, J. Geophys. Res., 87(B9), 7824–7827, 1982.

Gokhberg, M. B., Gershenzon, N. I., Gufeld, I. L., Kustav, A. V., Lipervsky, V. A., and Khusametdinov, S. S.: Possible effects of the action of Electric Fields of seismic origin on the ionosphere, Geomagnetism and Aeronomy, 24, 183–186, 1984.

Hayakawa, M. (Ed.): Atmospheric and ionospheric electromagnetic phenomena associated with earthquakes, Terra Scientific Publishing Company, Tokyo, 1999.

Hayakawa, M., Molchanov, O. A., and NASDA/UEC team: Achievements of NASDA's earthquake remote sensing frontier project, Terr. Atmos. Oceanic Sci., 15, 311–327, 2004.

Ishido, T. and Mizutani, H.: Experimental and theoretical basis of electrokinetic phenomena in rock-water systems and its applications to geophysics, J. Geophys. Res., 86, 1763–1775, 1981.

Izutsu, J.: Influence of lightning on the observation of seismic electromagnetic wave anomalies, Terr. Atmos. Ocean. Sci., 18, 923–950, http://tao.cgu.org.tw/pdf/v185p923.pdf, 2007.

Jackson, D. D. and Kagan, Y. Y.: Testable earthquake forecast for 1999, Seiesmo. Res. Lett., 70, 393–403, 1999.

Kapiris, P., Polygiannakis, J., Peratzakis, A., Nomicos, K., and Eftaxias, K.: VHF-electromagnetic evidence of the underlying pre-

seismic critical stage, Earth Planets Space, 54, 1237–1246, 2002.
Kikuchi, H.: Electrodynamics in dusty and dirty plasmas, Kluwer Academic Publishers, USA, 2001.
Kim, V. P. and Hegai, V. V.: On the possible changes in the mid-latitude upper ionosphere before strong earthquakes, J. Earthq. Predict. Res., 6, 275–280, 1997.
Kim, V. P. and Hegai, V. V.: The theoretical model of the possible changes in the nighttime mid-latitude D-region of the ionosphere over the zone of strong earthquake preparation, Radiophys. Quantum Radiophys., 45, 289–296, 2002.
Krider, E. P. and Roble, R. W. (Eds.): The Earth's Electrical Environment, National Academy Press, Washington D.C., 1986.
Liu, J. Y., Chuo, Y. J., Shan, S. J., Tsai, Y. B., Chen, Y. I., Pulinets, S. A., and Yu, S. B.: Pre-earthquake ionospheric anomalies registered by continuous GPS TEC measurements, Ann. Geophys., 22, 1585–1593, 2004,
http://www.ann-geophys.net/22/1585/2004/.
Molchanov, O. A. and Hayakawa, M.: Subionospheric VLF signal perturbations possibly related to earthquakes, J. Geophys. Res., 103, 17489–17504, 1998.
Molchanov, O. A., Hayakawa, M., and Rafalsky, V. A.: Penetration characteristics of electromagnetic emissions from an underground seismic source into the atmosphere, ionosphere, and magnetosphere, J. Geophys. Res., 100, 1691–1712, 1995.
MonaLisa, Kausar, A. B., Khwaja, A. A., and Jan, M. Q.: 8 October 2005 Pakistan earthquake: Preliminary observations and report of an international Conference at Islamabad, Pakistan, 18–19 January 2006, Episodes, 20, 5–7, 2006.
MonaLisa, Khwaja, A. A., and Jan, M. Q.: Seismic hazard assessment of the NW Himalayan Fold-and-Thrust Belt, Pakistan using probabilistic approach, J. Earthquake Eng., 11, 257–301, 2007.
MonaLisa, Khwaja, A. A., and Jan, M. Q.: The 8 October 2005 Muzaffarabad earthquake: Prelininary seismological investigations and probabilistic estimation of peak ground accelerations, Current Sci., 94, 1158–1166, 2008.
Nagao, T., Enomoto, Y., Fujinawa, Y., Hata, M., Hayakawa, M., Huang, Q., Izutsu, I., Kushida, Y., Maeda, K., Oike, K., Uyeda, S., and Yoshino, T.: Electromagnetic anomalies associated with 1995 KOBE earthquake, J. Geodynamics, 33, 401–411, 2002.
Ogata, Y.: Statistical model for standard seismicity and detection of Anomalies by Residual Analysis, Tectonophys., 169, 159–174, 1989.
Ogawa, T., Oike, K., and Miura, T.: Electromagnetic radiations from rocks, J. Geophys. Res., 90, 6245–6249, 1985.
Ohta, K., Umeda, K., Watanabe, N., and Hayakawa, M.: ULF/ELF emissions observed in Japan, possibly associated with the Chi-Chi earthquake in Taiwan, Nat. Hazards Earth Syst. Sci., 1, 37–42, 2001,
http://www.nat-hazards-earth-syst-sci.net/1/37/2001/.
Oike, K. and Ogawa, T.: Observations of electromagnetic radiation related with the occurrence of earthquakes. Ann. Rep., Disaster Prevention Res. Inst., Kyoto Univ., 25, 89–100, 1982.
Pathier, E., Fielding, E. J., Wright, T. J., Walker, R., Parsons, B. E., and Hensley, S.: Displacement field and slip distribution of the 2005 Kashmir earthquake from SAR imagery, Geophys. Res. Lett., 33, L20310, doi:10.1029/2006GL027193, 2006.
Pulinets, S. A.: Seismic activity as a source of the ionospheric variability, Adv. Space Res., 22(b), 903–906, 1998.
Pulinets, S. A., Legen'ka, A. D., Gaivoronskaya, T. V., and Depuev, V. K.: Main phenomenological features of ionospheric precursors of strong earthquakes, J. Atmos. Solar-Terr. Phys., 65(b), 1337–1347, 2003.
Rhoades, D. A. and Evison, F. F.: Long range earthquake forecasting with every earthquake a precursor according to scale, Pure Appl. Geophys., 161, 47–62, 2004.
Shanker, D., Yadav, R. B. S., and Singh, H. N.: On the seismic risk in the Hindukush-Pamir-Himalaya and their vicinity, Current Sci., 92, 1625–1630, 2007.
Shvets, A. V., Hayakawa, M., and Molchanov, O. A.: Subionospheric VLF monitoring for earthquake – related ionospheric perturbations, J. Atmos. Electricity, 22, 87–99, 2002.
Takeo, Y., Tomizawa, I., and Sugimoto, T.: Results of statistical analysis of LF seismogenic emissions as precursors to the earthquake and volcanic eruptions, Res. Lett. Atmos. Electr., 12, 203–210, 1992.
Yamada, T. and Oike, K.: Electromagnetic radiation phenomena before and after the 1995 Hyogo-ken Nanbu earthquake. J. Phys. Earth, 44, 405–412, 1996.
Yoshino, T. and Tomizawa, I.: Observation of low-frequency electromagnetic emissions as precursors to the volcanic eruption at Mt. Mihara during November, 1986, Phys. Earth Planet. Interiors, 57, 32–39, 1989.